Int J Wireless Inf Networks (2012) 19:173–184
DOI 10.1007/s10776-012-0189-x

Empirical Performance of RSSI-Based Monte Carlo Localisation for Active RFID Patient Tracking Systems

William P. L. Cully · Simon L. Cotton · William G. Scanlon

Received: 22 January 2012 / Accepted: 24 July 2012 / Published online: 10 August 2012

Abstract The range of potential applications for indoor and campus based personnel localisation has led researchers to create a wide spectrum of different algorithmic approaches and systems. However, the majority of the proposed systems overlook the unique radio environment presented by the human body leading to systematic errors and inaccuracies when deployed in this context. In this paper RSSI-based Monte Carlo Localisation was implemented using commercial 868 MHz off the shelf hardware and empirical data was gathered across a relatively large number of scenarios within a single indoor office environment. This data showed that the body shadowing effect caused by the human body introduced path skew into location estimates. It was also shown that, by using two body-worn nodes in concert, the effect of body shadowing can be mitigated by averaging the estimated position of the two nodes worn on either side of the body.

Keywords Localisation · Wearable · RSSI · Personnel · Monte Carlo · Body centric · ShadowingOff-body · Tracking

W. P. L. Cully · S. L. Cotton · W. G. Scanlon (✉)
The Institute of Electronics,
Communications and Information Technology,
Queen's University Belfast, NI Science Park,
Queen's Road, Queen's Island, Belfast, BT3 9DT, UK
e-mail: w.scanlon@qub.ac.uk
URL: www.ee.qub.ac.uk/wireless/

W. G. Scanlon
Telecommunication Engineering,
University of Twente, 7500 AE Enschede,
The Netherlands

1 Introduction

Active radio frequency identification (RFID) localisation systems have particular advantages for healthcare applications where knowledge of patient and employee movements and interactions can be used to improve overall organisational efficiency as well as quality of care. Substantial reductions in administrative costs may be achieved through automated data collection and monitoring in areas such as staff work patterns, processing of patients through triage, and ward or theatre utilization. Such a system will also ensure an appropriate frequency of staff and patient interactions, maintenance of adequate hygiene procedures, full traceability and an improved level of safety and security for both staff and patient.

Research interest into localisation systems has produced a wealth of positioning algorithms each with varying levels of complexity and infrastructural requirements. Much of this interest is due to the fact that determining the location of people within a building or other large area has many potential benefits and applications, such as assisting healthcare professionals within medical centres or maintaining security within transportation hubs.

Providing the location of people is challenging for any potential localisation scheme, not least because above all practical systems must be inexpensive and unobtrusive otherwise they would not see deployment nor would they be readily adopted by the users. Localisation based upon the received signal strength indicator (RSSI) is attractive then as RSSI values are routinely supplied by low power short-range wireless transceivers such as those found in active RFID systems.

In general, localisation systems determine the location of nodes by ranging, which is measuring the distance between adjacent nodes in the network, and then processing this data

to estimate positions. The RSSI can be used to give distance estimates by mapping the decay of radio signal strength but RSSI is not the only way to determine distance between nodes within a network. One of the most intuitive methods is to use time of arrival and measure the flight time of sent packets to determine the distance between sender and receiver, however this method requires synchronised nodes [1]. To overcome this drawback time difference of arrival may be used which measures the time taken to make a two way round trip between the nodes [2]. Time difference of arrival may also be provided by transmitting both radio and ultrasound signals at once with the difference in their propagation speeds creating a time difference that can be measured [3]. Of these methods RSSI is still the preferred method for sensing the environment, despite having the lowest reported accuracy of the methods mentioned [1], since its implementation requires no extra hardware other than the radios that are most likely already required by the desired application. For this reason the work presented here focussed on an RSSI based localisation scheme as it enabled implementation with inexpensive, off-the-shelf components.

The research into RSSI based localisation falls into two broad categories which are either range-free or range-based. Range-free methods are just a measure of connectivity that simply allows communicative nodes to know that the distance between each other is less than their maximum transmission range. Despite this coarse approach, much research has been carried out into using range-free methods which either define an area in which the node could be located, like centroid [4] and convex position optimisation [5] or use the geometry associated with a large number of network nodes such as ad hoc positioning system [6] or multidimensional scaling [7].

Range based methods remove the requirement for large numbers of nodes and may be invoked via simple trilateration [8], more complex procedures that account for channel variance [9] or by creating a signal strength map and referring to it when a position is needed [10]. The problem with these methods is that they do not explicitly account for node movement, which is important for the highly dynamic scenario of person localisation, unlike Monte Carlo localisation (MCL) [11] which incorporates node movement as a key principle of its operation. As a range-free localisation scheme MCL has seen a number of improvements that incorporate inferred orientation data [12], the position estimate of neighbouring nodes [13], or better error estimates [14]. In addition to these refinements there is also a range-based version, RSSI-based Monte Carlo localisation (RMCL) [15], which is implemented in this work and detailed in a later section.

For the localisation of people this still leaves the problem of complex and largely unpredictable radio wave interactions with the human body. While the effect of the user's orientation upon RSSI has been noted in the literature before [10], it has been largely overlooked in the design and implementation of localisation algorithms leading to inaccurate position estimates caused by body shadowing [16]. With this in mind this work gathered empirical data over a number of scenarios using commercial off-the-shelf hardware in order to establish the effect of the human body upon RSSI and ultimately the quality of the localisation estimates. This data was used to localise a person using RMCL with both the original data and with data modified by techniques designed to mitigate any deleterious effects caused by radio interactions with the body. To the best of the authors' knowledge this work is the only empirical study of multimode RMCL localisation for personnel localisation using multiple nodes. The work in this paper builds on, and is a significant advance over, the authors' previous work concerning single wearable node RMCL based personnel localisation [17].

This work is detailed in the subsequent sections as follows; an overview of RMCL is described in Sect. 2, while the testing environment and hardware are detailed in Sect. 3. In Sect. 4 the results from these experiments are presented and discussed. The final section closes with a conclusion and briefly outlines future work.

2 Algorithm Detail

2.1 Channel Model

The channel model used throughout this work was based on the log-distance path loss model. This is the one of the most common models found in localization literature and it is the model used in RMCL [15]. In this channel model the received power at a distance d is given as

$$\mathrm{RSSI}(d) = P_0 - 10n_p \log_{10}\frac{d}{d_0} + X_n \tag{1}$$

where P_0 is the reference power at a reference distance d_0 and n_p is the path loss exponent. In this model X_n signifies the noise component which is modelled as Gaussian with variance σ_n^2 and a mean of zero.

2.2 Overview of Monte Carlo Localization

The main idea behind MCL [11] is to represent the locations of the nodes within a network by a set of samples which cover possible locations that the node may occupy. With each new time step as the node moves a prediction is made as to the new location of the node by moving all the samples according to a transition distribution. The next step is filtering which removes all locations deemed impossible by the observations taken during the time step. Prediction

and filtering repeat in every time step taking the samples from the previous time step, moving, and refining them. With the range-free methods for MCL [11] filtering means removing samples by giving each sample a binary weighting of zero or one. While some schemes [13, 14] are able to add granularity to the weighting by estimating the accuracy of an individual node's position they still disregard information provided by the signal strength.

2.3 RSSI-based Monte Carlo Localization

RMCL [15] is able to utilise the information provided by signal strength by giving each sample point, $\theta_k^i = (x, y)$, an associated weight w_k^i. Where k is the time step, $i = 1,2,\ldots N_s$, and N_s is the total number of samples. At each new time step predictions are made based on the transition distribution $p(\theta_k|\theta_{k-1})$. As the subject's orientation is unknown and they may change direction between time steps the transition distribution is

$$p\left(\theta_k^i|\theta_{k-1}^i\right) = \begin{cases} \dfrac{1}{\pi d_{\max}^2}, & \text{dist}\left(\theta_k^i, \theta_{k-1}^i\right) \le d_{\max} \\ 0, & \text{dist}\left(\theta_k^i, \theta_{k-1}^i\right) > d_{\max} \end{cases} \tag{2}$$

where d_{max} is the maximum distance between sequential location predictions and $\text{dist}\left(\theta_k^i, \theta_{k-1}^i\right)$is the Euclidean distance between θ_k^i and θ_{k-1}^i. This makes any direction, within the radius $d_{\max}$, from the previous sample equally likely. After prediction the weight of each sample is calculated using

$$w_k^i = \frac{w_k^{*i}}{\sum_{j=1}^{N_s} w_k^{*j}} \tag{3}$$

where w_k^{*i} is the non-normalised weight. If one sets the transition prior as the importance density this allows recursive calculation of the non-normalized weight [18]. The non-normalised weight is then worked out with,

$$w_k^{*i} = w_{k-1}^{*i} p\left(m_k|\theta_k^i\right) \tag{4}$$

where $\mathbf{m}_k$ is the set of measurements made at time step k. The probability that a given signal strength is received at a certain distance is dependent upon the channel model and its noise characteristics. Using the model shown in (1) this probability is

$$p\left(P|d_{ij}\right) = \frac{1}{\sigma\sqrt{2\pi}} \exp\left\{ -\frac{P - P_0 + 10n_p \log_{10}\frac{d_{ij}}{d_0}}{2\sigma_n^2} \right\} \tag{5}$$

where P is the power received and d_{ij} is the distance between nodes i and j. With the samples and their associated weights calculated from previous equations the posterior distribution can be approximated as

$$p(\theta_k|m_{1:k}) \cong \sum_{i=1}^{N_s} w_k^i \delta\left(\theta_k - \theta_k^i\right) \tag{6}$$

where $\delta(\cdot)$ is the Dirac delta function. From this a single estimated location is chosen by taking the weighted mean of all the sample points,

$$\hat{\theta}_k = \sum_{i=1}^{N_s} \theta_k^i \cdot w_k^i. \tag{7}$$

However, RMCL can fall to the degeneracy problem, where all but one sample will have a negligible weight value. To avoid this the effective sample size is calculated using,

$$\widehat{N}_{\text{eff}} = \frac{1}{\sum_{i=1}^{N_s} \left(w_k^i\right)^2}. \tag{8}$$

If $\widehat{N}_{\text{eff}}$ is below the threshold value then systematic resampling [18] is applied and each sample weight is reset to $1/N_s$. Following [15] the threshold value is set at $N_s/10$. To start the algorithm $p(\theta_0)$ is initialised as a collection of random samples uniformly distributed throughout the sample area with all of their weights set to $1/N_s$. Starting from this RMCL predicts new locations and recalculates their weights in every new time step. Each time step is also accompanied with a check of the effective sample size, and the samples are resampled if necessary.

3 Experiment Overview

3.1 System Overview

The localisation system utilized within these experiments was based on *activ*Campus, a commercial active RFID localisation system supplied by ACT Wireless Ltd.[1] Within this system there were four *activ*Reader RFID reader units operating at 868 MHz and two wrist worn nodes (referred to as tags). The wrist-worn arrangement was chosen to be representative of potential healthcare applications where either patients or healthcare personnel are to be localized within medical facilities. The readers were stationary and placed in known locations within the test environment and so acted as anchor nodes. Based on the Texas Instruments CC1110 system on a chip transceiver,[2] the active RFID readers were set up to allow synchronous recording of RSSI levels at multiple readers during each interrogation with a range of −20 to −100 dBm and a resolution of 0.5 dBm for each 8 bit sample. All captured data was forwarded to a central server via Ethernet which enabled

[1] http://www.act-wireless.com

[2] http://www.ti.com/product/cc1110f32

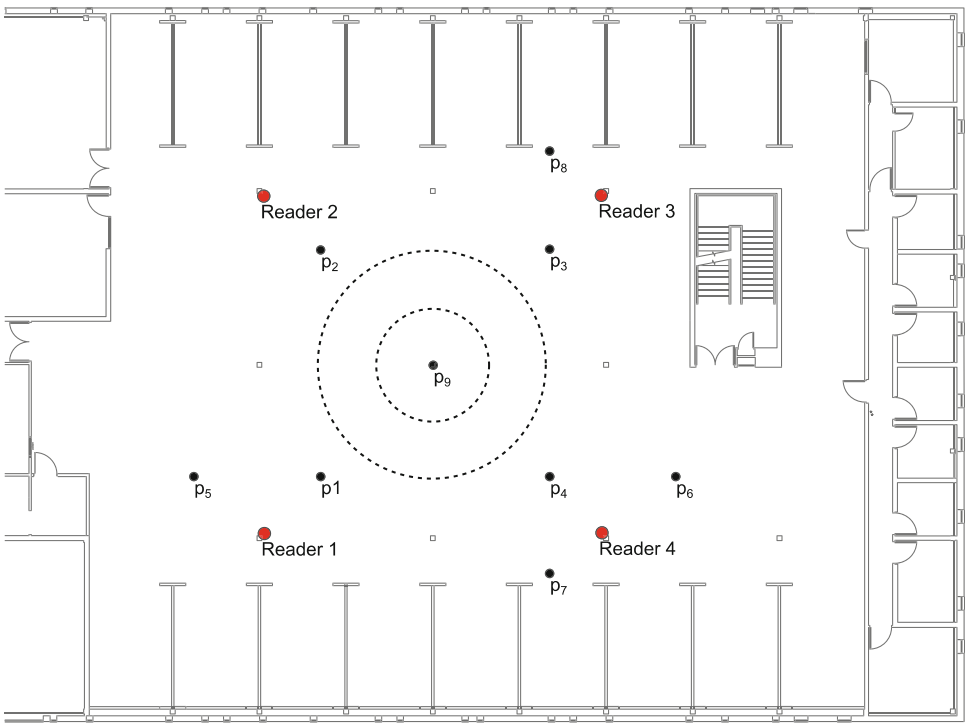

Fig. 1 Floor plan for the test environment, an open office environment at Queen's University Belfast incorporating four fixed readers, several trajectory 'points', p_1–p_9, and *dashed lines* illustrating the circular paths (full details are provided in Sect. 3 of the text)

analysis of the gathered data to be completed off-line during post processing.

The worn tags were a pair of eZ430-Chronos wrist-watch style wireless development systems from Texas Instruments which were programmed with custom firmware that enabled control of the packet rate while also incorporating a medium access control scheme that allowed the tags to transmit without interfering with each other by choosing a timeslot that minimised interference. The tags' individual interrogation rate was set at 8.33 Hz, allowing RSSI updates once every 120 ms from each tag.

3.2 Environment Overview

The experiments were conducted in a large open office space within the Old Science Library at Queen's University Belfast with a number of wooden partitions present along the long walls as shown in Fig. 1. Each partition had a height of 2.4 m and formed a cubicle containing computer workstations, chairs, desks, wooden shelves, and metal filing cabinets. The main experimental space was confined to the subset of this room as defined by the position of the four readers. The readers were mounted at a height of 2 m above the floor attached to support columns, forming a 14.4 × 14.4 m square. Both tags were worn by the same subject (height 1.75 m and weight 63.5 kg) for all of the measurement scenarios. Tag 1 was worn on the subject's left wrist, while Tag 2 was worn on the right wrist.

3.3 Scenario Description

Within the test environment eleven individual scenarios were considered with the path traced by the user following four basic shapes, a circle, a square, a straight line, and a horseshoe like shape. These scenarios are listed in Table 1. The data for each scenario was gathered over three trials with the first two runs being used exclusively for channel characterisation and reader calibration. The third run was reserved for testing the accuracy of the localisation scheme.

The circle and square paths were positioned so that the centre of each shape was aligned to the centre of the reader defined square. The two circular paths had radii of 3.25 and 6.5 m, with the center at point p_9. The circular paths were traversed in both clockwise and anticlockwise directions. There were also two separate square paths, the smaller of which was constructed of a square of side 9.5 m. The clockwise motion of this path was defined by the points p_1, p_2, p_3, p_4, p_1, see Fig. 1, while the anticlockwise was simply the reverse of this. The larger square path was the perimeter of the square enclosed by the readers and was also travelled in a clockwise and anticlockwise direction, starting at Reader 1. The horseshoe shape uses the same points as the smaller square, taking the path described by $p_1, p_2, p_3, p_4, p_3, p_2, p_1$. In following this path, the horseshoe incorporates both clockwise and anticlockwise motion in a single run. The two straight line scenarios were simply horizontal and vertical paths. The horizontal path was between p_5 and p_6, following

Table 1 Summary of measurement scenarios

Scenario	Shape	Details	Path
1	Circle	Radius = 3.25 m	Clockwise
2	Circle	Radius = 3.25 m	Anticlockwise
3	Circle	Radius = 6.5 m	Clockwise
4	Circle	Radius = 6.5 m	Anticlockwise
5	Square	Side = 9.5 m	Clockwise
6	Square	Side = 9.5 m	Anticlockwise
7	Square	Side = 14.4 m	Clockwise
8	Square	Side = 14.4 m	Anticlockwise
9	Horseshoe	Side = 9.5 m	$p_1, p_2, p_3, p_4, p_3, p_2, p_1$.
10	Straight Line	Horizontal	p_5, p_6, p_5
11	Straight Line	Vertical	p_7, p_8, p_7

Table 2 Summary of the measured channel parameters used by each reader

Reader	P_0	n_p	σ_n^2
1	−49.2	1.28	4.69
2	−50.4	1.36	4.43
3	−52.1	1.52	5.35
4	−56.9	0.82	5.47

the path p_5, p_6, p_5. Similarly the vertical path follows the path described by p_7, p_8, p_7.

4 Results

To account for any manufacturing variance the channel parameters were determined on a per reader basis. Table 2 summarises the channel parameters as calculated by MATLAB using least squares estimation of the measured trajectories in the first and second trial runs. When compared to the channel parameters used in previous simulated work [15] it can be seen that in the empirical data not only is there a greater variance, and therefore more noise, but also smaller values of n_p which means that for any change in signal strength the effect on the estimated distance will be greater.

The RSSI data gathered from the tags was processed in four different ways, resulting in four different localisation estimates. These were based on:

- Tag 1 only,
- Tag 2 only,
- RSSI averaged from Tag 1 and Tag 2, or
- Position averaged from Tag 1 and Tag 2 estimations.

In more detail the first localisation source was the signal strength using data gathered only from Tag 1 and the second used the signal strength data from just Tag 2. The third method averaged the signal strength data from both tags. The final method involved independently localising both tags and then averaging these two positions to produce a final position estimate. The RSSI used within each time step of RMCL was made up of the mean power received in a window of 12 samples long (1.44 s) and each time step was separated by 4 samples (0.48 s). In all cases the window and step size were the same. To gauge the effectiveness of using RMCL with these various localisation estimates, the error values for each scenario were calculated in each time step as the Euclidean distance between the estimated location supplied by RMCL and the true location taken from known trajectory and time data. These results are summarised in Table 3 which shows the root mean square (RMS), mean, and 50th percentile error values for all of the scenarios. These values are calculated from a total of 1000 RMCL algorithm iterations for each scenario. Table 3 also provides the measured walking pace for the user, calculated from time measurements and the distance travelled.

Initial examination of the data shows that overall it is, as expected, less accurate than reported simulation results [15]. This is due to the combined outcome of the less than favourable channel model parameters, with lower path loss exponent and higher noise, and the effects of human body shadowing. These results are also less accurate than other empirical measurements made using real people [17], but the main difference is that this work was conducted at an average user speed that is almost twice as fast as [17] and with a wider reader coverage area of almost 52 m^2 versus 30 m^2, and so larger errors are to be expected.

It is also worth noting that in all except two scenarios, all of the metrics used to evaluate the performance of RMCL were in agreement about the most accurate form of localisation estimate, e.g., mean position or mean RSSI. So while RMS error may be the preferred metric for localisation, as it more readily accounts for large but infrequent errors, for the purposes of assessing the relative accuracy of localisation methods any of the stated metrics may be used. This can be readily observed in Fig. 2 which shows the cumulative distribution function (CDF) of the localisation error in Scenario 6 and is typical of the error distributions seen in all scenarios. As well as showing the improvement in localisation accuracy achieved by combining the data from both tags, Fig. 2 also illustrates how one tag can provide a better location estimation than the other tag. This is due to body shadowing and is explored in the remainder of this section.

Table 3 Localisation error statistics for each scenario and each localisation source (individual tag, mean RSSI or mean position)

Scenario	Location source	RMS error (m)	Mean error (m)	50th Percentile error (m)	Average speed (m/s)
1	Tag 1	4.51	4.26	4.26	1.08
	Tag 2	**3.37**	**2.98**	**2.79**	
	Mean RSSI	3.42	3.19	3.07	
	Mean Position	3.46	3.29	3.12	
2	Tag 1	3.09	2.65	2.33	1.08
	Tag 2	2.62	2.42	2.40	
	Mean RSSI	2.34	2.09	1.97	
	Mean Position	**2.13**	**1.85**	**1.63**	
3	Tag 1	2.89	2.52	2.32	1.04
	Tag 2	3.61	3.21	3.00	
	Mean RSSI	2.79	2.46	2.27	
	Mean Position	**2.59**	**2.27**	**2.06**	
4	Tag 1	4.66	4.34	4.11	1.08
	Tag 2	3.66	3.37	3.20	
	Mean RSSI	**3.46**	**3.24**	**3.15**	
	Mean Position	3.69	3.52	3.39	
5	Tag 1	3.74	3.37	3.22	1.11
	Tag 2	3.65	3.04	**2.53**	
	Mean RSSI	3.43	2.91	2.60	
	Mean Position	**3.25**	**2.73**	2.57	
6	Tag 1	3.22	2.95	2.86	1.08
	Tag 2	2.83	2.57	2.50	
	Mean RSSI	2.57	2.33	2.23	
	Mean Position	**2.49**	**2.25**	**2.11**	
7	Tag 1	2.56	2.14	1.90	1.18
	Tag 2	3.11	2.59	2.28	
	Mean RSSI	2.53	2.08	1.79	
	Mean Position	**2.35**	**1.99**	**1.79**	
8	Tag 1	3.17	2.86	2.75	1.17
	Tag 2	2.77	**2.43**	**2.32**	
	Mean RSSI	2.86	2.55	2.46	
	Mean Position	**2.70**	2.46	2.40	
9	Tag 1	2.94	2.59	2.37	1.10
	Tag 2	3.45	2.92	2.58	
	Mean RSSI	3.10	2.66	2.34	
	Mean Position	**2.92**	**2.49**	**2.17**	
10	Tag 1	3.59	3.20	2.98	1.10
	Tag 2	3.24	2.80	2.53	
	Mean RSSI	3.15	2.72	2.48	
	Mean Position	**3.03**	**2.60**	**2.31**	
11	Tag 1	5.50	4.63	3.82	1.06
	Tag 2	**3.29**	**3.12**	**3.10**	
	Mean RSSI	3.78	3.46	3.11	
	Mean Position	3.87	3.53	3.15	

Table 3 continued

Scenario	Location source	RMS error (m)	Mean error (m)	50th Percentile error (m)	Average speed (m/s)
All	Tag 1	3.63	3.13	2.86	N/A
	Tag 2	3.26	2.85	2.69	
	Mean RSSI	3.06	2.68	2.50	
	Mean Position	**2.98**	**2.61**	**2.44**	

The best results for each scenario and metric are shown in *bold*

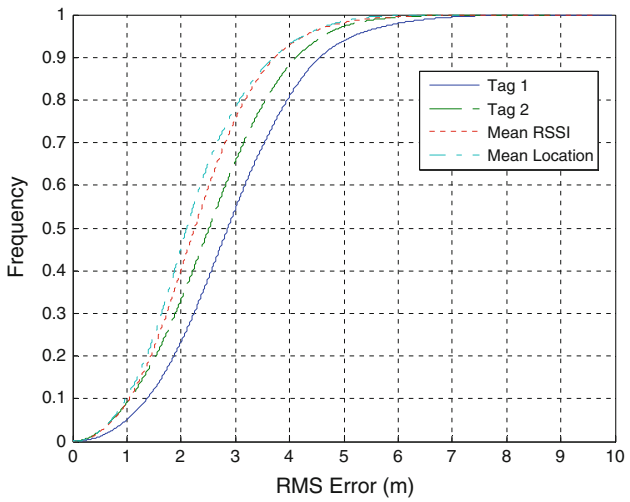

Fig 2 CDF showing the distribution of RMS error in Scenario 6

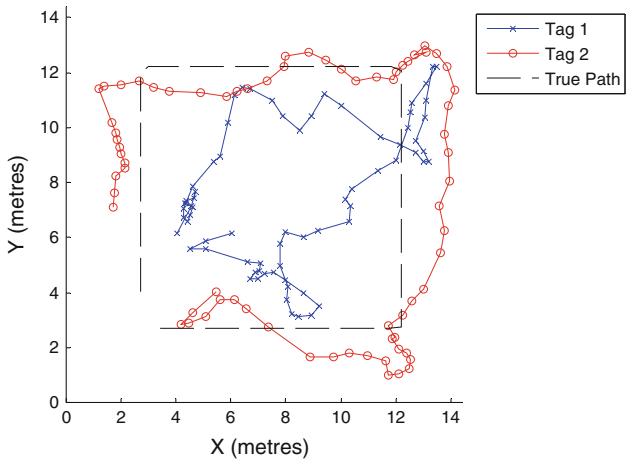

Fig. 3 Estimated user trajectories for Scenario 6, where the user travels anticlockwise in a *square*

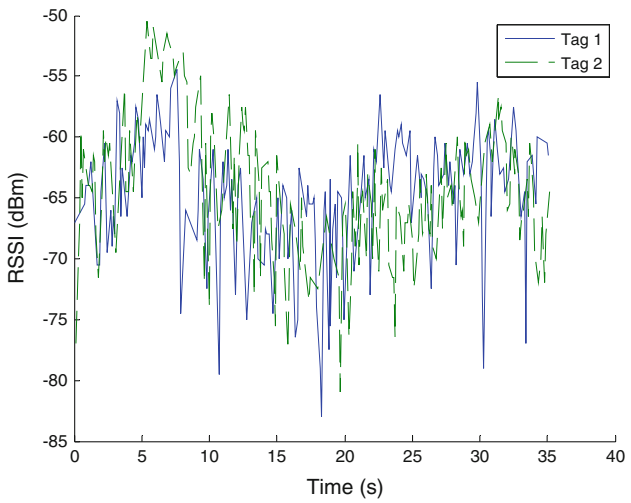

Fig. 4 Time series of the RSSI measured at Reader 4 from both tags during Scenario 6

4.1 Tag Location and Body Shadowing

The placement of the tag on the body is an important consideration as human body shadowing can strongly affect the accuracy of signal strength based localisation schemes. In the experiments conducted here, this led to a worst case scenario of a 67 % increase in the RMS error. Closer inspection of the estimated user trajectories provided by RMCL shows that human body shadowing can introduce a skewing effect that causes a constant path deviation. An example of this is shown in Fig. 3 which displays the estimated paths for Scenario 6, where the subject travelled along a square path in an anticlockwise direction. In Fig. 3 the path estimated using only RSSI data for Tag 2 tends to fall outside of the square defined by the true path, whereas the path for Tag 1 tends to be within the square defined by the true path.

This observed skew was caused by the body shadowing effect in which the body blocks of the line of sight (LOS) between the tag and the readers. As Tag 2 was worn on the right wrist during the anticlockwise path of this scenario, it had an unobstructed LOS to whichever reader the subject was closest to. Conversely, Tag 1 had a non-line of sight (NLOS) path to the closest reader as the user's body was blocking the path at all times. The effect of the NLOS path is shown in Fig. 4 which displays the RSSI measured at Reader 4 (bottom right corner, Fig. 1) during Scenario 6. It can be seen that at the peak RSSI level, when the user was closest to the reader, the signal strength from Tag 1 was lower than was measured from Tag 2.

The lower signal strength provided by the NLOS path causes an overestimation of the distance between the closest tag and the reader which leads to an estimated location that is skewed towards the centre of the testing area and away from the reader. While Tag 1 was able to maintain a LOS path to the more distant readers, the ranging estimate provided by the RSSI for the other readers would still be less accurate due to the much lower signal levels.

To combat the body shadowing effect and provide more accurate location estimates two different methods of combining data from both tags were tested. In the first method the gathered RSSI values from the two tags were pooled and averaged within one localisation window. This combined RSSI value was determined on a per-reader basis and used for the RMCL localisation estimate at that particular time-step. The second method was to average the independent position estimates obtained using RMCL for an individual tag at each time-step.

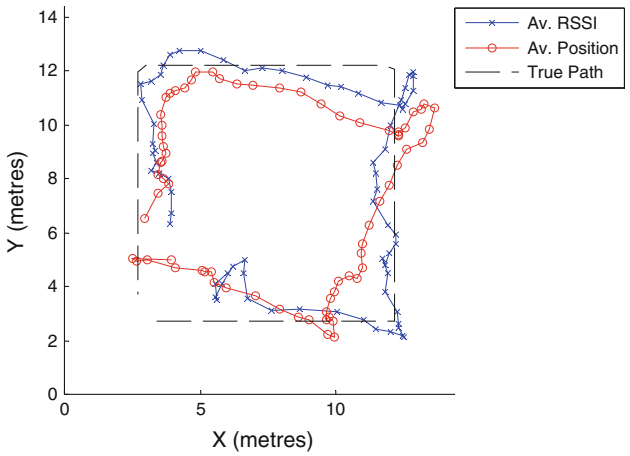

Fig. 5 Estimated user trajectories for Scenario 6 when using the average RSSI and the average position to provide location estimates at each time-step

The effect of combining the data like this is displayed in Fig. 5 which shows a typical path generated from the average RSSI and average position localisation sources in Scenario 6. These localisation sources result in paths that are closer to the true path and individual position estimates that are more evenly separated, more closely representing the constant walking pace of the user.

The observed body shadowing effect persisted in all tested scenarios although it was not always as simple as skewing the estimated path off of the true path. Inspection of the estimated trajectories produced in the worst performing scenario, which was Scenario 4 where the user walked anticlockwise in a large circle, showed that a skew due to body shadowing was present but it was not centred about the true path, as shown in Fig. 6.

Inspection of the RSSI time series for Scenario 4 revealed a dramatic fade at approximately 15 s into the scenario, see Fig. 7a. This prolonged fade allowed for a distance estimate at that time of nearly 150 m which is several times larger than expected (Fig. 7b). For comparison the distance estimates between Tag 1 and Reader 2 are displayed in Fig. 7c, showing that such extreme overestimates are rare. That fact that this reader was unable to cause a large deviation in the path of Tag 1 shows the robust nature of RMCL over other memoryless localisation algorithms.

Despite the overall poorer performance for Scenario 4, the effect of averaging the RSSI data from the tags produced more accurate results. This was similar to the improvements observed for Scenario 6 (see Fig. 5), were the combined data localisation sources produce paths that are more accurate, with more evenly spaced position estimates, and with fewer large deviations.

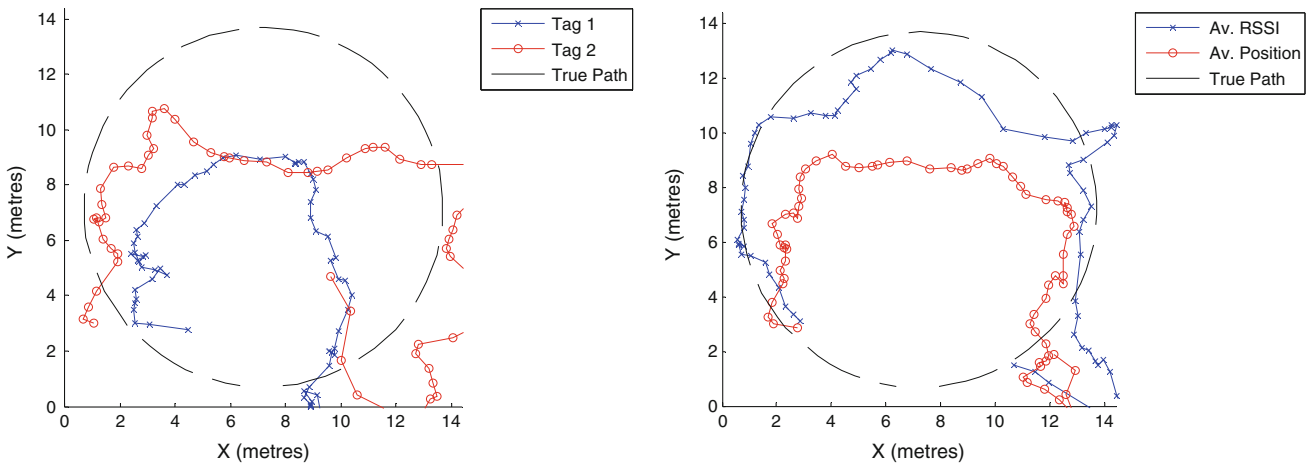

Fig. 6 Estimated user trajectories for Scenario 4 for all four localisation sources (each individual node, average RSSI and average position)

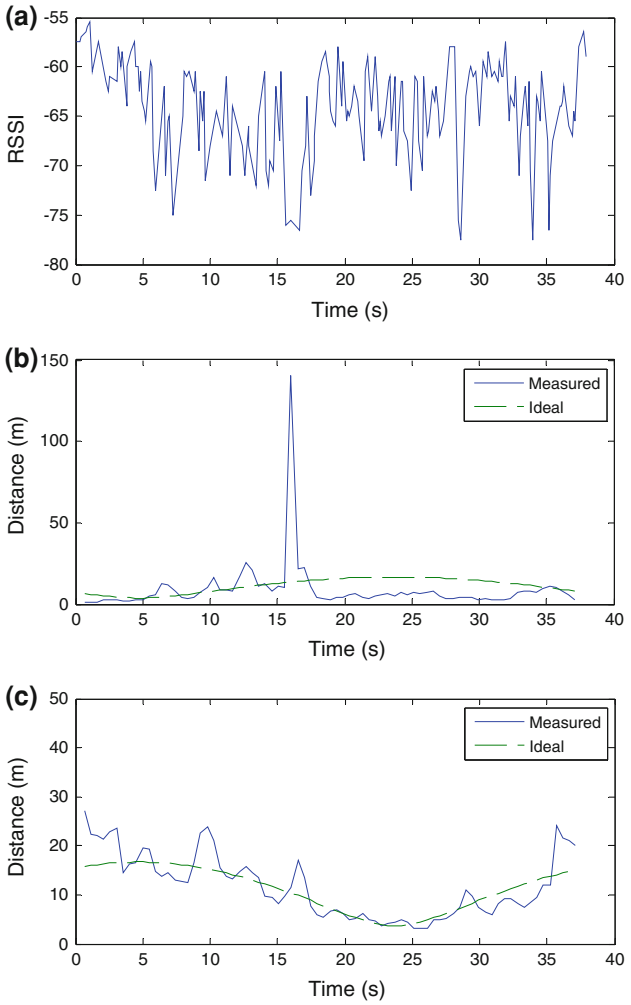

Fig. 7 Time series of **a** RSSI from Tag 1 recorded at Reader 4 and the estimated distance between Tag 1 and **b** Reader 4 and **c** Reader 2

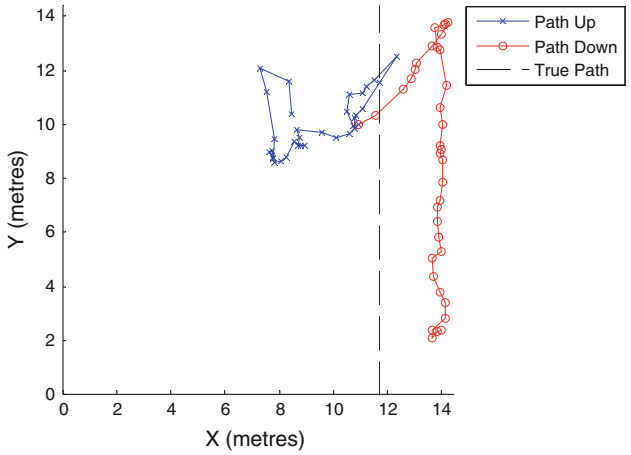

Fig. 8 Estimated user trajectories for Tag 1 in Scenario 11, where the user followed a *straight line* up and down the testing area

This qualitative assessment of the improvement is supported by the summary error statistics presented in Table 3. It can be observed that while both methods of error mitigation offer an accuracy improvement, the average position method provided the most accurate localisation method in the majority of scenarios. The main exception was in Scenario 11, although this result may be explained via observation of the RSSI levels and noting their resulting effect upon the location estimation. For Scenario 11 an unusually low signal level was measured by Reader 1 from Tag 1 at the very start of the experiment which caused an initial location that was skewed towards the centre of the testing area, as can be seen in Fig. 8. Since RMCL uses previous location estimates to generate new locations this error is propagated through several time steps. It should be noted that even after the recovery of the position estimate, the path skew due to body shadowing observed in Fig. 3 is still present and forces the position estimate off the true path. In Fig. 8 this can be seen on the downwards estimated path where it is skewed to the right of the true path.

Despite this outlying scenario the results in Table 2 illustrate that it is still advantageous to use the average position of both tags as the user's location. This is in contrast to the findings of [19] which show that the average RSSI is a better means of combining data from multiple tags. However, the tags in [19] were kept at a fixed distance from one another whereas in this work they were wrist-mounted on a human frame resulting in a dynamic and constantly changing separation distance. For this body-centric scenario the average position is the best localisation technique as during a standard human gait (where one arm is in front of the body and the other is symmetrically behind) despite the changing separation, the mean position of the two tags will always be at the centre of the user's body. Not only is it the most accurate location estimate in the majority of cases but choosing this localisation method will allow one to calculate a position estimate without having to determine the LOS condition of the tag in each time step and then compensate for it. While knowledge of the LOS status between the node and reader allows for greater accuracy [17] this improvement needs to be weighed against the additional complexity and processing that a NLOS compensation system would require.

4.2 Initialisation Phase

Aside from errors directly related to body interaction there are other errors associated with MCL. The start up error seen in Scenario 11 is a common phenomenon exhibited in many MCL systems [11–14]. Termed as the initialisation phase, this is the period of time in which the location error starts off relatively high but decreases as new observations are incorporated. Although not all initialisation phases are

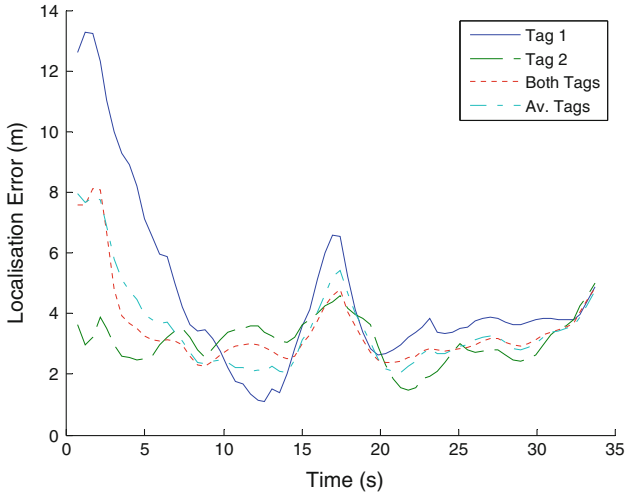

Fig. 9 Time series of the average error over 1000 RMCL runs for Scenario 11 illustrating how an inaccurate starting location can lead to residual errors

Table 4 RMS error for all the scenarios in both RMCL and Seeded RMCL

Localisation method	Tag 1	Tag 2	Mean RSSI	Mean position
RMCL	3.63	3.26	3.06	2.98
Seeded RMCL	3.26	2.96	2.78	2.72
Improvement (%)	10	9	9	9

as dramatic as those seen in Scenario 11, see Fig. 9, all of the tested scenarios suffer from this to some extent.

This initialisation phase could potentially lead to increased error levels if used within the framework of a more extensive localisation system where each individual room or area would have their own set of readers. In such a system the initialisation phase would occur every time the user enters a new localisation area, defined by the boundaries of each room or subsections of a larger area due to partition shadowing or limits on received signal strength due to limited transmit power in wearable and portable devices. There are a number of methods one could use to alleviate this problem, ranging from a trilateration scheme which is activated as the user passes chokepoints such as the entrance to a room to the use of a map of the building with known location of entrance and exit points. To investigate the benefit of implementing this type of scheme a variant of RMCL was evaluated in which the known starting location was seeded into the localisation system at the first time step. Table 4 shows the RMS error of RMCL and Seeded RMCL taken over 1,000 trials of all of the scenarios.

From Table 4 it can be seen that Seeded RMCL performs better overall for every localisation source although its effectiveness decreases for the combined sources. This shows that a component of the error observed in the initialisation phase is due to the effect of the human body and can be partially overcome by application of body shadowing mitigation techniques.

5 Conclusions and Future Work

In this paper an implementation of RMCL was presented that employed commercial off-the-shelf hardware that enabled the collection of empirical data for personnel localisation within a typical operating environment. Investigation of this data showed that the position of the tag upon the user is an important consideration with regards to localisation accuracy due to the body shadowing effect. Body shadowing causes a reduction in signal strength for the LOS path between the tags and the readers which leads to an overestimation of this distance resulting in a constant path skew that was observed in all scenarios. Techniques to compensate for the path skew caused by body shadowing have been presented. These have shown that taking the average position of the two tags offered the most accurate location estimate for the majority of the scenarios considered here. This was because the tags were situated on opposite wrists which meant that the path skew for each was in opposing directions.

These positive results have illustrated the potential of the stated approach and it is the intention of the authors to conduct additional experiments to further establish the robustness of this location estimator, particularly in more complicated environments. With regards to the algorithm itself, future work into RMCL for body-centric applications will involve adaptation specifically for wearable multi node applications such as body area networks. Here, the use of multiple nodes could lead to the generation of a confidence measure for each position estimate and providing this to subsequent time steps. For example, considering the two node example presented in this paper, this confidence measure may be computed by evaluating the Euclidian distance between the estimated position of Tag 1 and Tag 2. The closer their positions are, the more confident the system can be about this position estimate as their proximity is indicative of reliable ranging from each reader for each tag.

Acknowledgments This work was supported in part by a research studentship from the Centre for Secure Information Technology, Institute of Electronics, Communications and Information Technology, Queen's University Belfast. The author's are grateful to ACT Wireless Limited for supplying equipment and data acquisition software, and are grateful to Dr. Adrian McKernan of ACT Wireless who assisted with the measurements.

References

1. A. Boukerche, H. Oliveira, E. Nakamura and A. Loureiro, Localization systems for wireless sensor networks. *IEEE Wireless Communications*, Vol. 14, No. 6, pp. 6–12, 2007.
2. N. Patwari, J. N. Ash, S. Kyperountas, A. O. Hero, R. L. Moses and N. S. Correal, Locating the nodes: cooperative localization in wireless sensor networks. *IEEE Signal Processing Magazine*, Vol. 22, No. 4, pp. 54–69, 2005.
3. N. B. Priyantha, A. Chakraborty, and H. Balakrishnan, The Cricket location-support system. *Annual International Conference on Mobile Computing and Networking*, pp. 32–43, 2000.
4. N. Bulusu, J. Heidemann and D. Estrin, GPS-less low-cost outdoor localization for very small devices. *IEEE Personal Communications*, Vol. 7, No. 5, pp. 28–34, 2000.
5. L. Doherty, K. S. J. Pister and L. El Ghaoui, Convex position estimation in wireless sensor networks. *IEEE International Conference on Computer Communications*, Vol. 3, pp. 1655–1663, 2001.
6. Niculescu, D., and Nath, B. Ad hoc positioning system (APS), *Global Telecommunications Conference (GLOBECOM)*, pp. 2926–2931, 2001.
7. Y. Shang, and W. Ruml, Improved MDS-based localization. *IEEE International Conference on Computer Communications*, pp. 2640–2651, 2004.
8. P. Motter, R.S. Allgayer, I. Muller, C.E. Pereira, and E. Pignaton de Freitas, Practical issues in Wireless Sensor Network localization systems using received signal strength indication. *IEEE Sensors Applications Symposium*, pp. 227–232, 2011.
9. C.-H. Chang, and W. Liao, Revisiting relative location estimation in wireless sensor networks. *IEEE International Conference on Communications*, pp. 1–5, 2009.
10. P. Bahl, and V. N. Padmanabhan, RADAR: an in-building RF-based user location and tracking system. *Proceedings of 19th Annual Joint Conference of the IEEE Computer and Communications Societies*, Vol. 2, pp. 775–784, 2000.
11. L. Hu, and D. Evans, Localization for mobile sensor networks. *Proceedings of the 10th annual international conference on Mobile computing and networking*, pp. 45–57, 2004.
12. M.H.T. Martins, H. Chen, and K. Sezaki, OTMCL: Orientation tracking-based Monte Carlo localization for mobile sensor networks. *International Conference on Networked Sensing Systems*, pp. 1–8, 2009.
13. M. Rudafshani, and S. Datta, Localization in wireless sensor networks. *International Conference on Information Processing in Sensor Networks*, pp. 51–60, 2007.
14. S. Zhang, J. Cao, C. Li-Jun and D. Chen, Accurate and energy-efficient range-free localization for mobile sensor networks. *IEEE Transactions on Mobile Computing*, Vol. 9, No. 6, pp. 897–910, 2010.
15. W. D. Wang and Q. X. Zhu, RSS-based Monte Carlo localisation for mobile sensor networks. *IET Communications*, Vol. 2, No. 5, pp. 673–681, 2008.
16. W.P.L. Cully, S.L. Cotton, W.G. Scanlon, and J.B. McQuiston, Localization algorithm performance in ultra low power active RFID based patient tracking. *22nd IEEE International Symposium on Personal, Indoor & Mobile Radio Conference* (*PIMRC*), Toronto, Canada, pp. 2303–2307, 2011.
17. W.P.L. Cully, S.L. Cotton, W.G. Scanlon, and J.B. McQuiston, Body shadowing mitigation using differentiated LOS/NLOS channel models for RSSI-based Monte Carlo personnel localization. *IEEE Wireless Communications & Networking Conference* (*WCNC 2012*), Paris, France, 2012.
18. M. S. Arulampalam, S. Maskell, N. Gordon and T. Clapp, A tutorial on particle filters for online nonlinear/non-Gaussian Bayesian tracking. *IEEE Transactions on Signal Processing*, Vol. 50, No. 2, pp. 174–188, 2002.
19. C. Guo, J. Wang, R.V. Prasad, and M. Jacobsson, Improving the accuracy of person localization with body area sensor networks: An experimental study. *2009 6th IEEE Consumer Communications and Networking Conference*, pp. 1–5, 2009.

Author Biographies

William P. L. Cully received his masters degree (with honours) in Electrical and Electronic Engineering from Queen's University Belfast, UK in 2010. He is presently studying for his Ph.D. in electronic engineering at the Centre for Secure Information Technology, ECIT Institute. His current research interests include personal localisation and off body channel modelling.

Simon L. Cotton received the B.E. degree in electronics and software from the University of Ulster, Ulster, UK, in 2004 and the Ph.D. degree in electrical and electronic engineering from the Queen's University of Belfast, Belfast, UK, in 2007. Since graduating, Dr Cotton has worked as a Research Fellow and Senior Research Fellow at Queen's University Belfast, where he has investigated mobile ad hoc networking of dismounted combat personnel and low power personnel and asset tracking using RFID. He is currently a Lecturer at Queen's and he is also a cofounder and the Chief Technology Officer at ACT Wireless Ltd. In April 2010 he was awarded a highly prestigious 5 year Research Fellowship from the Royal Academy of Engineering to investigate next generation body centric communications. Among Dr Cotton's current research interests are millimetre-wave technologies for personal communications and novel applications of short-range radio systems including body-to-body networking and vehicular communications. His other research interests include radio channel characterization and modelling for wireless body and personal area networks, measurements for transceiver diversity in bodyworn applications and simulation of wireless channels. He has authored and co-authored over 46 publications in major IEEE/IET journals and refereed international conferences, one book chapter and two patents. Dr. Cotton has been the recipient of a number prominent awards including the H.A. Wheeler Prize from the IEEE Antennas and Propagation Society in July 2010, the Sir George Macfarlane Award

from the Royal Academy of Engineering and a Philip Leverhulme Prize from the Leverhulme Trust in July and October 2011, respectively.

William G. Scanlon received the B.E. degree in electrical engineering and the Ph.D. degree in electronics (specializing in wearable and implanted antennas) from the University of Ulster, UK in 1994 and 1997, respectively. He was appointed as Lecturer at the University of Ulster in 1998, Senior Lecturer and Full Professor at Queen's University of Belfast (UK) in 2002 and 2008, respectively. He is currently Chair of Wireless Communications and Director of Research for the Digital Communications Cluster at Queen's and he holds a part-time Chair in Short Range Radio at the University of Twente, The Netherlands. Prior to starting his academic career he had 10 years of industrial experience, having worked as a Senior RF Engineer for Nortel Networks, as a Project Engineer with Siemens and as a Lighting Engineer with GEC-Osram. His current research interests include personal and body-centric communications, wearable antennas, RF and microwave propagation, channel modelling and characterization, wireless networking and protocols and wireless networked control systems. He has published approximately 200 technical papers in major IEEE/IET journals and in refereed international conferences. He served as keynote speaker for the NATO Military Communications and Information Systems Conf. (2010), the Intl. Conf. on Bodynets (2010) and the European Workshop on Conformal Antennas (2007). He also Co-Chaired the 2009 Loughborough Antennas and Propagation Conference and he has acted as invited speaker and session chair at numerous other national and international conferences. Prof. Scanlon received a Young Scientist award from URSI in 1999, and he was a recipient of the 2010 IEEE H. A. Wheeler Prize Paper Award and he is also a prolific reviewer for IEEE/IET journals and major conferences. He was a founding Director of WirelessLAB (Ireland) and is currently a founding Director and Chief Scientist of ACT Wireless Limited, a member of the IEEE International Committee on Electromagnetic Safety (ICES) and the IASTED International Committee on Telecommunications.